JOC The Journal of Organic Chemistry

Article

pubs.acs.org/joc

Stereochemical Outcome of Copper-Catalyzed C−H Insertion Reactions. An Experimental and Theoretical Study

Gonzalo Jiménez-Osés,*[,†] Eugenio Vispe,[‡] Marta Roldán,[‡] Sergio Rodríguez-Rodríguez,[‡,§] Pilar López-Ram-de-Viu,[‡] Luis Salvatella,[‡] José A. Mayoral,[‡] and José M. Fraile*[,‡]

[†]Department of Chemistry and Biochemistry, University of California, Los Angeles, Los Angeles, California 90095-1569, United States

[‡]Instituto de Síntesis Química y Catálisis Homogénea, Facultad de Ciencias, Universidad de Zaragoza-CSIC, 50009 Zaragoza, Spain

Supporting Information

ABSTRACT: The combination of chiral preparative HPLC separation, VCD measurements, and theoretical calculations allows the unambiguous determination of the absolute configuration of the conformationally flexible products of copper-catalyzed carbene insertion reactions. DFT calculations were used to predict the stereochemical outcome of the copper-bis(oxazoline)-catalyzed C−H insertion reaction between methyl diazophenylacetate and tetrahydrofuran and also to predict the absolute configuration of the major stereoisomers derived from the same reaction with different cyclic ethers. These predictions were verified experimentally through NMR and VCD spectroscopy and allowed rationalization of the stereochemical outcome of these reactions without further derivatization of the products, which can be prblematic under certain conditions as described herein.

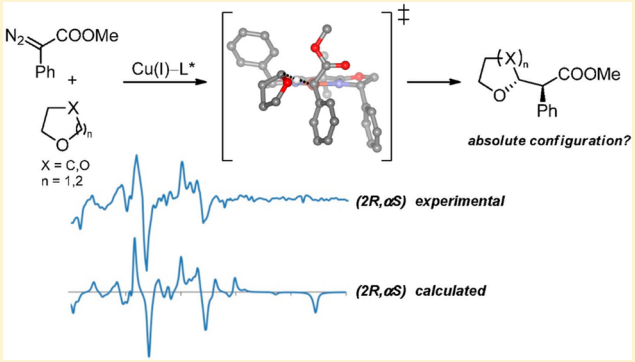

INTRODUCTION

Despite the great success achieved in the preparation of enantiopure compounds, for which asymmetric catalysis has played a key role, the determination of the absolute configuration of *each* stereogenic center present in the new molecule remains frequently elusive despite achieving a highly stereoselective synthesis or an exhaustive purification.[1] When X-ray diffraction analysis or derivatization to known compounds is not feasible, relative configurations and very scarcely absolute configurations can be directly inferred by spectroscopic techniques like NMR, polarimetry, and electronic or vibrational circular dichroism (ECD[2,3] or VCD,[4] respectively). Together with the development of these experimental techniques, the theoretical prediction of magnetic, optical, electronic, and vibrational properties of chemical compounds has emerged as a powerful tool in the recent years. Particularly, VCD spectroscopy,[4] which is based on vibrational absorptions effected by polarized radiations, benefits from many advantages, being applicable to virtually all chiral compounds. VCD spectra are more complex and provide much more structural information than ECD and are less influenced by solvent effects.[5] Additionally, the theoretical prediction of VCD properties is performed in the ground (i.e., nonexcited) electronic state and is less method-dependent than ECD. Altogether, these advantages of VCD spectroscopy have contributed to its rapid expansion within the organic community. In this context, valuable efforts pioneered by Stephens et al. have been performed recently to elucidate the absolute configuration of complex natural and, to a lesser extent, synthetic products and metal complexes with excellent results.[2,5−34]

However, the theoretical prediction of any molecular property, especially the spectroscopic ones, and the subsequent comparison with experimental results suffer from a very serious drawback: it can be performed straightforwardly only for quite *rigid* compounds. In these situations, an excellent agreement between experimental and theoretical calculations can be achieved. Otherwise, the experimental values and spectra are the result of the combination of the individual contributions from all the conformers present in solution, which are generally explored within the acquisition time scale. In these situations, theory can provide reliable results only if all the possible conformers are calculated and their properties are weighted with their relative population under the experimental conditions.[29,32,34] Despite the increasing capability of modern theoretical methods to accurately compute spectroscopic properties, even for large systems, the high complexity arising from highly fluxional compounds has seriously limited its application to real-life synthetic derivatives, and this computational task is still challenging. Thus, an accurate description of the conformational space of such compounds must be done prior to the calculation of the spectroscopic properties. This can be of particular importance when coexisting conformers display opposite properties (vide infra).

Received: February 28, 2013
Published: May 23, 2013

In this sense, the enantioselective insertion reaction of formal carbenes into C−H bonds constitutes a major challenge in current organic synthesis.[35,36] Pioneering work by Davies et al. has contributed to the rapid development of this chemistry, in which high enantioselectivities have been reached using chiral rhodium catalysts.[37,38] Alternatively, our group has recently reported an arguably green procedure based on the use of copper complexes in the homogeneous or heterogeneous phase (Scheme 1).[39−41]

Scheme 1. Reactions between Methyl Diazophenylacetate and Cyclic Ethers Catalyzed by Chiral Copper Complexes[a]

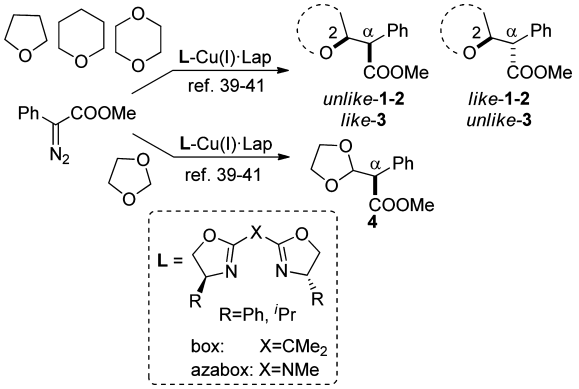

[a]Lap = Laponite (heterogeneous support).

Good levels of stereoselection were achieved in the reaction of methyl diazophenylacetate with tetrahydrofuran (THF) using bis(oxazoline) (box) and azabis(oxazoline) (azabox) ligands bearing phenyl and isopropyl groups (up to 64% enantiomeric excess (ee) in the major diastereomer), the effect of immobilizing the catalyst onto an inorganic support being remarkable (up to 88% ee in the major diastereomer). However, only the *relative* configuration of the C_α and C2 atoms of **1** could be deduced from ^{1}H NMR experiments for each of the diastereomeric pairs (*unlike* and *like*). The absolute configuration of each stereocenter could not be unambiguously determined, and only the stereochemistry of the major *unlike* insertion product could be tentatively assigned as (2*R*,α*S*) through the qualitative coincidence of its specific optical rotation ($[\alpha]_D^{25}$ = −88.1) with previously reported values for the same ($[\alpha]_D^{25}$ = −74.0)[42] and opposite ($[\alpha]_D^{25}$ = +68.4)[43] enantiomers.

This methodology was extended to similar cyclic ethers, namely tetrahydropyran (THP), 1,4-dioxane, and 1,3-dioxolane, to successfully obtain compounds **2**, **3** (obtained under both homogeneous and heterogeneous conditions), and **4** (obtained only in heterogeneous phase), respectively (Scheme 1), with moderate to good yields and stereoselectivities (up to 56−71% ee depending on the substrate). To the best of our knowledge, the stereoselective preparation of these derivatives has not been reported to date, precluding the comparison of their optical/spectroscopic properties with reference data. As in the case of THF-derived compounds, the relative configuration of each pair of enantiomers was established by NMR experiments on the basis of previous studies reported by Davies et al.[44] Again, the *unlike* (2*R*,α*S* and 2*S*,α*R*) isomers were the major products for the reaction with THP. On the contrary, and due to the change in priority of the substituents attached to C2, the *like* (2*S*,α*S* and 2*R*,α*R*) enantiomers were dominant when the reaction was conducted with 1,4-dioxane. The diastereomeric ratios in all cases ranged from 50/50 to 75/25. In the case of the reaction with 1,3-dioxolane, only one stereogenic center is formed.

Until now, no reliable structural information on the source of the enantioselectivities of such processes has been available. This is a major drawback not solved to date which limits the high potential of these reactions. In this study, we combine spectroscopic and theoretical techniques to establish, for the first time, the stereochemical outcome of this reaction.

RESULTS AND DISCUSSION

All attempts to obtain single monocrystals of any of the oily products, either from enantioenriched mixtures of enantiomers or even from pure enantiomers (see below), were unsuccessful. In situations in which the only information available is a set of peaks in a HPLC trace, one of the strategies to assess the stereochemistry of each product, and subsequently the course of the asymmetric induction, is to determine which compounds have the same configuration at a given stereocenter.

For example, the absolute configuration of the major *like*-**1** enantiomer may be determined by epimerization of the major *unlike*-**1** enantiomer, taking advantage of the presence of an acidic hydrogen at the α position of these enolizable compounds. This epimerization should lead to diastereomers with identical configuration at C2. These experiments are thoroughly described in the Supporting Information, and only the most significant results will be described herein.

Hence, epimerization assays on C_α were performed on enantioenriched samples of *unlike*-**1**, where we assumed the configuration of the major enantiomer is **1**-(2*R*,α*S*) as proposed by Davies.[42] Treatment with different bases and under different conditions led to a mixture of the four stereoisomers. Under equilibrium conditions, the *unlike*/*like* ratio was completely reversed with respect to the catalytic results, showing that the *like* diastereomer is more thermodynamically stable than the *unlike* product, which is in good agreement with subsequent theoretical calculations (vide infra). Strikingly, the enantiomeric purity was completely lost, suggesting that not only the α position bearing the acidic hydrogen but also the one adjacent to the endocyclic oxygen (C2) was subjected to reaction upon basic treatment.

Because the simultaneous enolization of the C2 position was ruled out by additional assays performed in deuterated solvents, a different mechanism for this transformation must be invoked. The base-promoted retro-*O*-Michael reaction occurring in related oxazolidines bearing alkyl esters and leading to α,β-unsaturated compounds has been described.[45−48]

Scheme 2. Proposed Ring-Opening/Cyclization Mechanism for the Base-Promoted Racemization of C_α and C2 in Compound 1

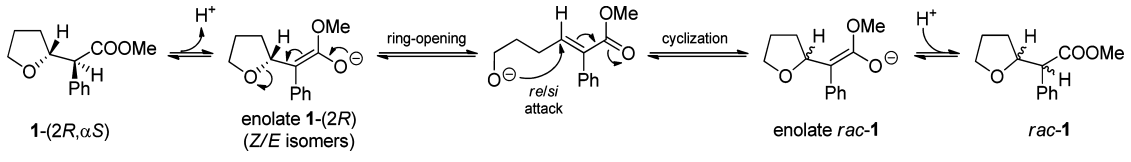

dx.doi.org/10.1021/jo400415b | J. Org. Chem. 2013, 78, 5851−5857

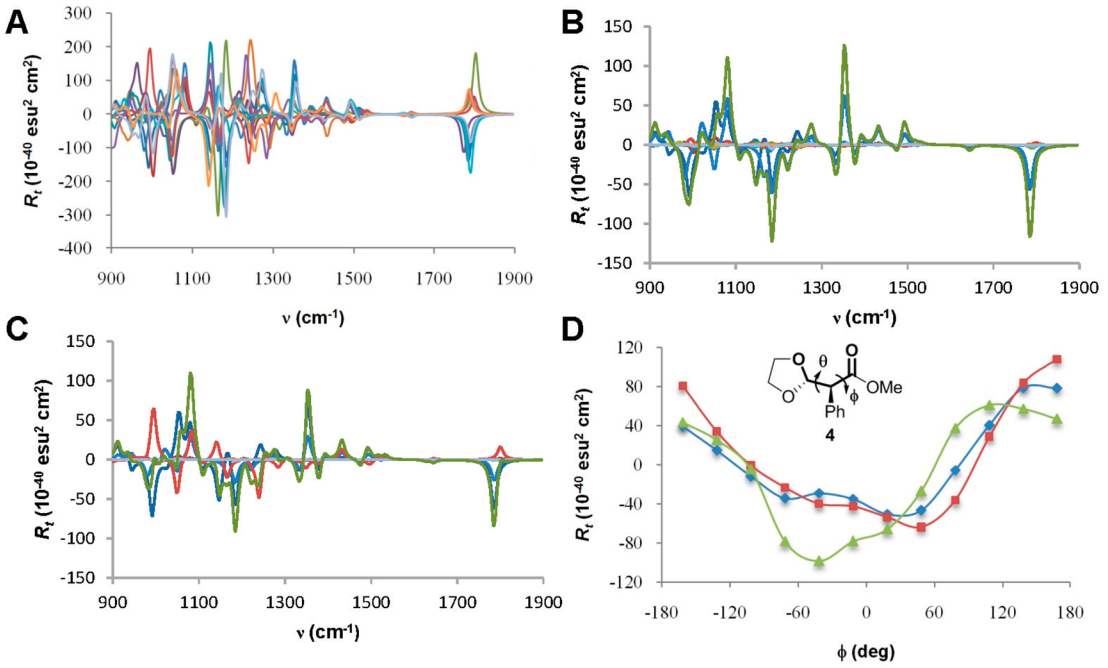

Figure 1. (A–C) Overlay of the theoretical VCD spectra calculated for each of the 13 conformers of compound **4**-(*S*) optimized at the B3LYP/TZVP level. (A) Conformationally unweighted in the gas phase (global spectrum in green). (B) Conformationally weighted in the gas phase (global spectrum in green). (C) Conformationally weighted in chloroform solution. (D) Plot of calculated R_t (CO st) vs ϕ dihedral angle for three different rotamers of **4**-(*S*) ($\theta \simeq 60°$ in blue, $\theta \simeq 180°$ in red, $\theta \simeq -60°$ in green). VCD calculations were performed at the B3LYP/TZVP level. In all cases, the resolution (half-width at half-height) of the spectra is 8 cm^{-1}.

We propose that a ring-opening/cyclization cascade reaction takes place together with the simple epimerization of C_α upon treatment of ester **1** with a base (Scheme 2).

However, under milder conditions, the *like*-**1** product was obtained with a significant enantiomeric excess, **1**-(2*R*,α*R*) being the major product, probably due to the fact that the protonation of enolate **1**-(2*R*) is faster than the ring-opening process (Scheme 2). From this identification of the *like* enantiomers, the major *like*-**1** product of the insertion reaction can be tentatively assigned to **1**-(2*S*,α*S*).

These results revealed that the configurational stability of chiral activated cyclic ethers can be seriously affected under certain conditions, precluding the experimental determination of their absolute configuration by selective epimerization, derivatization, and so forth. In these situations, spectroscopic and theoretical methodologies are required to confidently assess the stereochemistry of the resulting products.

VCD Spectroscopy. Both enantiomers of the major *unlike*-**2** and *like*-**3** pairs and both enantiomers of **4** were isolated by semipreparative chiral HPLC (Experimental Section). The VCD spectra of the six enantiopure compounds were collected (see Experimental Section). In some cases, the spectra of two enantiomers were not exact mirror images, which was attributed to small concentration differences and baseline effects.[49]

The experimental data were compared to those predicted theoretically. In order to select the most convenient methodology, three different levels of theory (B3LYP/6-31G(d), B3LYP/TZVP, and B3PW91/TZVP) were previously tested. As can be seen in Figure S3 in the Supporting Information, the B3LYP functional achieved the best performance, in terms of both the energy and intensity associated with the different vibrations. According to previous results,[21−26] a triple-ζ basis set is required to accurately reproduce the experimental spectra.

The proper description of the dominant conformations in such flexible compounds is a key issue in accurately reproducing the observed spectroscopic properties. This fact is clearly illustrated in Figure 1A, which shows the radically different calculated spectra of all conformers of **4**-(*S*). The geometries and relative population of these conformers are shown in Figure S2 in the Supporting Information. The relative populations of each conformer derived from their relative free Gibbs energies (Δ*G*) through a Boltzmann distribution at 25 °C were used to scale their corresponding spectra. The sum of all contributions was used to obtain the final theoretical spectra that were compared to those measured experimentally. As can be seen in panels B and C of Figure 1, in these systems, the contribution of solvation effects (chloroform) on the relative population of each conformer and thus on the global theoretical spectrum is negligible.

A detailed inspection of the individual spectra associated with each conformer reveals that the positive or negative values of the rotational strength (R_t) of each vibration depend not only on the absolute configuration of the stereogenic carbon but also on the relative orientation of each functional group. It is worth noting that the free rotations or conformational changes of some functional groups have a more pronounced effect on the energy and intensity of their associated vibrations than a change of configuration at remote stereogenic centers. To further illustrate this observation, Figure 1D shows the high variability of the calculated rotational strengths of the carbonyl stretching vibration (CO st 1775−1800 cm^{-1}) of compound **4**-(*S*) along the dihedral ϕ. In view of these results, only a careful evaluation of the conformational energies and a subsequent weighting of each spectrum can lead to satisfactory conclusions.

In view of these preliminary results, a combinatorial evaluation of both the relative energies and the VCD properties of all the conceivable conformers of each enantiomer of *unlike*-**2**, *like*-**3**, and **4**

dx.doi.org/10.1021/jo400415b | J. Org. Chem. 2013, 78, 5851−5857

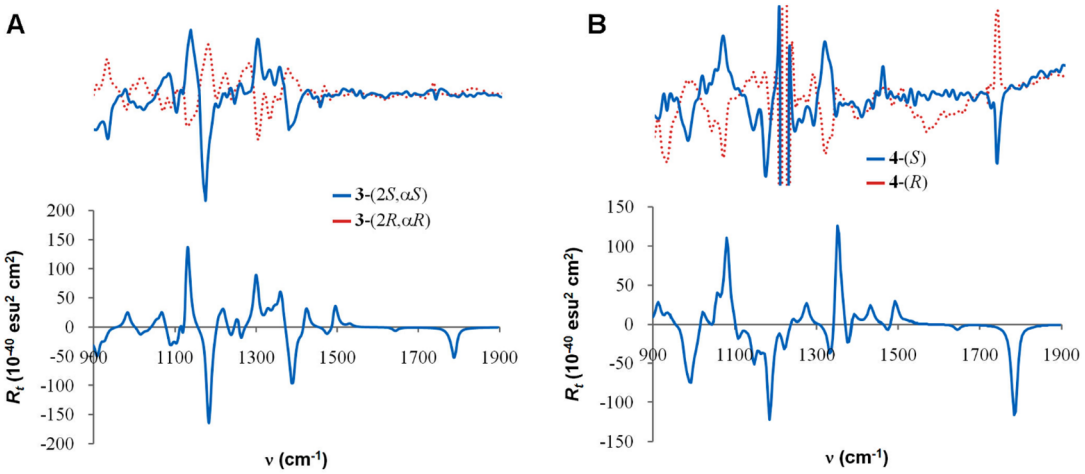

Figure 2. (A) Experimental VCD spectra of both *like*-**3** enantiomers (upper panel) and conformationally weighted theoretical VCD spectrum of **3**-(2S,αS) (lower panel). (B) Experimental VCD spectra of both enantiomers of compound **4** (upper panel) and conformationally weighted theoretical VCD spectrum of **4**-(*S*) (lower panel). VCD calculations were performed at the B3LYP/TZVP level. Solvent ($CHCl_3$) interference is observed in the 1205−1225 cm^{-1} region. In all cases, the resolution (half-width at half-height) of the spectra is 8 cm^{-1}.

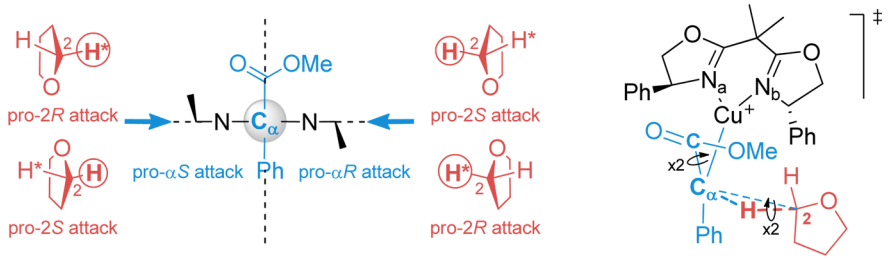

Figure 3. Geometric features and reaction trajectories considered for the calculation of all TS's of the Cu(I)-catalyzed reaction of methyl diazophenylacetate with THF.

was done (Figure S3 in the Supporting Information). The comparison of the conformationally weighted theoretical and experimental VCD spectra of both enantiomers of *like*-**3** and **4** reveals remarkably good agreement between both sets of data (panels A and B of Figure 2, respectively) when bearing in mind all the fluxionality drawbacks mentioned above.

The experiments and calculations performed throughout this study allowed us to definitely establish the absolute configuration of the major C−H insertion products as (2*R*,αS) in the case of reaction with THP, (2*S*,αS) with 1,4-dioxane, and (*S*) with 1,3-dioxolane. These results agree with the configuration proposed by Davies for the major insertion product derived from THF.[42] Thus, a steady induction of asymmetry toward an (*S*) configuration of C_α has been observed in the Cu(I)-catalyzed reaction of methyl diazophenylacetate with cyclic ethers in the presence of (*S*)-(bis)oxazolines.

Theoretical Studies on the C−H Insertion Mechanism. Aside from the experimental verification of the absolute configuration of the reaction products, the theoretical prediction of the most favorable pathways is a powerful tool to gain insights into the stereochemical course of a given reaction and the asymmetry induction mechanisms, particularly in metal-carbenoid processes in which the stereoselective step is hidden by the rate-limiting step such as in this type of C−H insertion reactions (i.e., formation of the carbenoid).[50,51] To this end, we performed a theoretical analysis of all the possible reaction pathways for a model C−H insertion reaction. In our previous reports, we described the copper-catalyzed C−H insertion of diazo compounds into several cyclic ethers in the presence of box and azabox ligands.[39−41] For the calculations, we selected THF as the model substrate and the box(Ph) ligand bearing phenyl groups at the oxazoline rings (Figure 3).

A total of 16 transition states (TS's), resulting from the combination of four geometric features including stereoisomers and conformers (Figures 2 and S3 in the Supporting Information), were located and characterized. The contribution of each TS was quantified by a Boltzmann distribution at 66 °C based on B3LYP-D3/6-31G(d) zero-point corrected electronic energies (Table 1).

The most stable arrangement for each stereoisomeric approximation is shown in Figure 4. All calculated geometries and a more detailed description of their geometric features are summarized in Figure S4 and Table S1 in the Supporting Information. All transition structures show a quasi-linear hydride transfer from THF C2 to the copper−carbene complex C_α ($C2^{\cdots}H^{\cdots}C_\alpha$ = 147−161°), leading to two formal moieties (oxolan-2-yl carbocation and a neutral organocopper species), which recombine in a highly asynchronous but concerted way as previously reported by theoretical studies on alkane C−H carbene insertion reactions catalyzed by copper[52,53] and rhodium.[54] The presence of an incipient carbocation in the TS's agrees with several Hammett studies on metal-catalyzed C−H carbene insertion reactions.[55−57]

Systematic differences between pro-αR and pro-αS approximations can be observed. Thus, whereas the THF attack took place through the catalyst equatorial plane (N_a−Cu=C_α···C2 torsion angle absolute value > 168°) in the pro-αS approximation, a significant deviation is found for the pro-αR attack (N_a−Cu=C_α···C2 torsion angle = 145−164°).

dx.doi.org/10.1021/jo400415b | J. Org. Chem. 2013, 78, 5851−5857

Table 1. Calculated B3LYP-D3/6-31G(d) Energies and Stereoisomeric Distribution at 66 °C Derived from C−H Insertion Transition States TS1

structure	ΔE_{ZPE} (kcal mol^{-1})	mol %	cumulative mol %	experimental ratio[a]
TS1-(2*R*,α*S*) alkoxy_O-in	3.2	0.3	66.5	50.9
TS1-(2*R*,α*S*) alkoxy_O-out	0.0	35.2		
TS1-(2*R*,α*S*) oxy_O-in	1.9	2.0		
TS1-(2*R*,α*S*) oxy_O-out	0.1	29.1		
TS1-(2*S*,α*S*) alkoxy_O-in	5.2	0.0	27.4	25.2
TS1-(2*S*,α*S*) alkoxy_O-out	1.0	8.2		
TS1-(2*S*,α*S*) oxy_O-in	5.1	0.0		
TS1-(2*S*,α*S*) oxy_O-out	0.4	19.2		
TS1-(2*R*,α*R*) alkoxy_O-in	5.1	0.0	4.5	10.8
TS1-(2*R*,α*R*) alkoxy_O-out	2.3	1.1		
TS1-(2*R*,α*R*) oxy_O-in	4.7	0.0		
TS1-(2*R*,α*R*) oxy_O-out	1.6	3.4		
TS1-(2*S*,α*R*) alkoxy_O-in	3.4	0.2	1.5	13.1
TS1-(2*S*,α*R*) alkoxy_O-out	5.5	0.0		
TS1-(2*S*,α*R*) oxy_O-in	3.9	0.1		
TS1-(2*S*,α*R*) oxy_O-out	2.3	1.2		

[a]Obtained with box(Ph) ligand in homogeneous phase.[39]

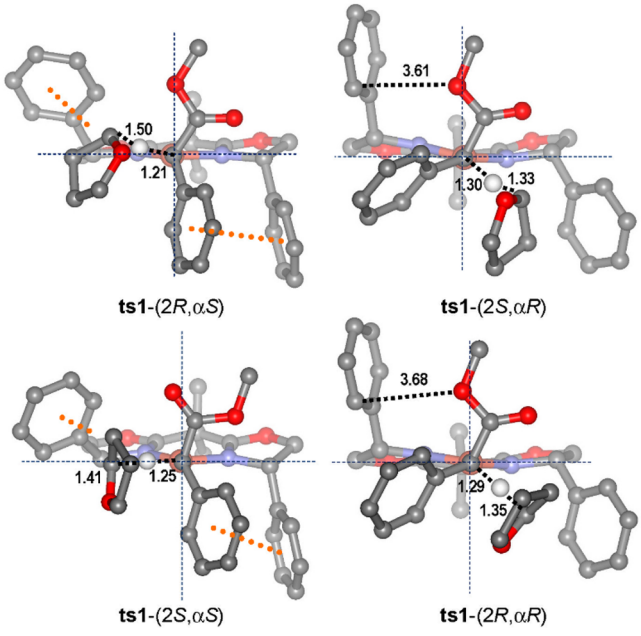

Figure 4. B3LYP-D3/6-31G(d) minimum energy geometries of the four stereoisomeric TS's for the Cu−carbene complex insertion reaction with THF (TS1). Distances are given in angstroms, and van der Waals interactions are qualitatively depicted as orange lines.

Such systematic α*R* vs α*S* differences are attributed in part to the steric repulsions occurring between the ester group and the oxazoline substituent. Such steric repulsions are originated by the C_α partial sp^2 to sp^3 rehybridization, which is analogous to our reaction model of a cyclopropanation reaction catalyzed by the same copper complex.[58,59] These destabilizing contacts confer on all pro-α*R* TS's a substantial conformational stress, reducing the stereodiscrimination between the pro-2*R* and pro-2*S* pathways, which is higher in the less hindered pro-α*S* approximations.

Significantly, the experimental trend is reproduced only when an empirical correction to dispersion (D3)[60] is added to the energy of each TS. Otherwise, the (2*S*,α*S*) stereoisomer is predicted to be favored by about 2 kcal mol^{-1}, which is in disagreement with the experimental results. This result reinforces the importance of van der Waals interactions in systems in which a number of hydrophobic contacts can take place. Particularly, π−π interactions between the oxazoline and carbene phenyl rings, and also CH−π interactions between the other oxazoline phenyl ring and the tetrahydrofuran moiety, are apparent (3.2−3.4 Å) in the pro-α*S* approximations and probably contribute to the stabilization of these pathways.

As summarized in Table 1, the calculated contributions of each stereoisomer are in good agreement with the product distribution obtained experimentally in the presence of box(Ph) ligand. However, this fairly good correlation is obtained only when *all* TS's are calculated and included in the Boltzmann distribution, because several reactive approximations are nearly isoenergetic and contribute almost equally to the final mixture. This issue is of major importance when evaluating the mechanisms of asymmetry induction, especially when the stereoselectivity is not excellent. In such cases, overlooking just one reaction pathway can change the predicted stereoselectivity dramatically.

Finally, and as a complement to the kinetic stereoselectivity predicted through the calculated TS's, the thermodynamic stability of the products was evaluated at the same theoretical level. In sum, up to 12 *unlike* and 10 *like* conformers were calculated for each stereoisomer. A very low *unlike/like* calculated ratio (0.97) was obtained through a Boltzmann distribution of the relative electronic energies of all conformers (Table S2 in the Supporting Information). This value is opposite to the kinetic distribution obtained both experimentally and theoretically, and in a good agreement with the results obtained during prolonged treatment of **1** with base.

In summary, the computational investigation of all conceivable reaction pathways for the copper-carbene insertion into THF confirmed the high propensity of (*S*)-bis(oxazoline) ligands to promote pro-α*S* asymmetric induction due to steric interactions between the carbene ester group and the alkyl/aryl substituent of the oxazoline. The *unlike/like* diastereomeric ratio was also predicted correctly, as was the high enantioselectivity in favor of the (2*R*,α*S*) enantiomer.

■ CONCLUSIONS

When highly flexible products are obtained, the spectroscopic determination of their absolute configuration is a very challenging task. In such cases, VCD spectroscopy in combination with rigorous quantum mechanics calculations provides a very useful methodology.

In this work, a synergistic experimental and theoretical study on the copper-catalyzed C−H insertion of diazo compounds into cyclic ethers allowed the confident elucidation of the stereochemical

dx.doi.org/10.1021/jo400415b | J. Org. Chem. 2013, 78, 5851−5857

course of this reaction, which has been found to be general for a series of related substrates.

Following the same trend exhibited by bis(oxazoline)−Cu(I) complexes in the asymmetric cyclopropanation of olefins, the highly asynchronous concerted carbene insertion takes place preferably by the *re* face of the Cu(I)−carbene system. The source of the observed stereoselection arises from a balance of stereoelectronic factors in which the repulsive interactions between the ester group and the alkyl/aryl groups of the oxazoline rings, and also the attractive van der Waals interactions between the substrates and the ligand, play major roles.

In epimerization studies, performed by basic treatment of activated cyclic ethers, the absolute configuration of all the stereogenic centers present on the molecule is affected through a proposed ring-opening/cyclization process, leading to a complete loss of asymmetry. These findings are a caveat for chemical derivatization, a common strategy for the elucidation of stereochemical induction.

EXPERIMENTAL SECTION

Bisoxazolines,[61] azabisoxazolines,[62−64] and supported catalysts[39−41,62] were prepared as described in the literature. The copper-catalyzed reactions of methyl diazophenylacetate with cyclic ethers and the reaction products have been described elsewhere.[39−41]

Preparative Chiral HPLC. ***Compound 2.*** Column: Chiralpak IA 2 × 25 cm. Eluent: *n*-hexane/ethanol (99.8/0.2), 16 mL/min. Sample: 90 mg of *unlike*-**2** + *like*-**2** previously purified by silica gel column chromatography. Sample concn: 100 mg/mL. Injections: 0.1 mL. Retention times: **2**-(2*R*,*αS*), 8.4 min; **2**-(2*S*,*αR*), 9.5 min; *like* product (enantiomer 1), 10.4 min; *like* product (enantiomer 2), 12.1 min. Yields: 20 mg of **2**-(2*R*,*αS*) $[\alpha]_D^{25} = -76.4°$ (*c* 0.55, CCl_4); 30 mg of **2**-(2*S*,*αR*) $[\alpha]_D^{25} = +78.2°$ (*c* 0.75, CCl_4). ***Compound 3.*** Column: Chiralpak IB 2 × 25 cm. Eluent: *n*-hexane/acetone (98/2), 20 mL/min. Sample: 206 mg of *unlike*-**3** + *like*-**3** previously purified by silica gel column chromatography. Sample concn: 160 mg/mL. Injections: 0.1 mL. Retention times: *unlike*-**3** (enantiomer 1), 15.4 min; *unlike*-**3** (enantiomer 2), 16.2 min; **3**-(2*R*,*αR*), 17.4 min; **3**-(2*S*,*αS*), 21.0 min. Yields: 40 mg of **3**-(2*R*,*αR*) $[\alpha]_D^{25} = +50.6°$ (*c* 0.575, $CHCl_3$); 48 mg of **3**-(2*S*,*αS*) $[\alpha]_D^{25} = -46.6°$ (*c* 0.585, $CHCl_3$). ***Compound 4.*** Column: Chiralpak IB 2 × 25 cm. Eluent: *n*-hexane/acetone (99/1), 20 mL/min. Sample: 118 mg. Sample concn: 50 mg/mL. Injections: 0.1 mL. Retention times: **4**-(*R*), 32.4 min; **4**-(*S*), 34.2 min. Yields: 10 mg of **4**-(*R*) $[\alpha]_D^{25} = -40.4°$ (*c* 0.65, $CHCl_3$); 20 mg of **4**-(*S*) $[\alpha]_D^{25} = +41.4°$ (*c* 0.95, $CHCl_3$).

Racemization Assays. ***Method 1a.*** Compound **1**-(2*R*,*αS*) (40 mg, 0.18 mmol) was dissolved in dry methanol (1 mL), and NaOMe (0.5 M in methanol, 0.72 mL, 0.36 mmol) was added; the mixture was stirred at room temperature for 24 h. ***Method 1b.*** Compound **1**-(2*R*,*αS*) (10.5 mg, 0.048 mmol) was dissolved in dry methanol (0.5 mL), and NaOMe (0.5 M in methanol, 76 μL, 0.038 mmol) was added; the mixture was stirred at room temperature for 24 h. ***Method 1c.*** Compound **1**-(2*R*,*αS*) (9.8 mg, 0.045 mmol) was dissolved in dry methanol-d_4 (0.7 mL), and solid NaOMe (2 mg, 0.036 mmol) was added; the mixture was stirred at room temperature for 24 h. ***Method 2.*** Compound **1**-(2*R*,*αS*) (10 mg, 0.045 mmol) was dissolved in dry toluene (0.5 mL), and 1,3,5-triazabicyclodec-5-ene (TBD) bound to polystyrene (13.8 mg, 0.036 mmol) was added; the mixture was stirred at room temperature for 5 days. In all experiments, the reaction was monitored by HPLC (Chiralpak IB 0.46 × 25 cm) using *n*-hexane/isopropanol (99.5/0.5, 0.8 mL/min) as eluent. Retention times: **1**-(2*R*,*αS*), 12.0 min; **1**-(2*S*,*αR*), 13.1 min; **1**-(2*S*,*αS*), 16.1 min; **1**-(2*R*,*αR*), 17.3 min.

VCD Spectroscopy. Experiments were carried out in solution on a Jasco FVS-4000 spectrometer using a cell equipped with BaF_2 windows and a 0.1 mm spacer. Samples were dissolved in CCl_4 or $CHCl_3$ to get an IR absorbance close to 0.4, and then 2000 scans were collected in the range of 900−1800 cm^{-1} at a resolution of 8 cm^{-1}. Then spectra were corrected using the solvent as baseline.

Computational Methods. All calculations reported in this paper were performed within the density functional theory. The B3LYP functional[65,66] was used for all geometry optimizations. The 6-31G(d) and TZVP basis sets were used for geometry optimizations and the calculation of frequencies and VCD properties.[67] BSSE corrections were not considered in this work. All the stationary points located were characterized by the correct number and nature of their imaginary frequencies. Scaled frequencies were not considered. Bulk solvent effects were considered implicitly by performing single-point energy calculations on the gas phase optimized geometries, through the SMD polarizable continuum model of Cramer and Thrular[68] as implemented in Gaussian 09. The internally stored parameters for chloroform were used to calculate solvation free energies (ΔG_{solv}). Electronic energies including Grimme's empirical correction to dispersion[60] and Gibbs free energies (ΔG) were used throughout the discussion. In all cases, the Gaussian 09 suite of programs was used.[69] Full details on calculated structures and energies can be found in the Supporting Information.

ASSOCIATED CONTENT

Supporting Information

Detailed description of specific experiments and theoretical models; NMR and HPLC data of compounds **2**−**4**; tables of geometric features, electronic energies, and enthalpies, entropies, and Gibbs free energies for the different conformations of the structures considered in this work; calculated geometries of the structures discussed in this paper; and additional figures and tables. This material is available free of charge via the Internet at http://pubs.acs.org.

AUTHOR INFORMATION

Corresponding Author

*E-mail: G.J.-O., gjimenez@chem.ucla.edu; J.M.F., jmfraile@unizar.es.

Present Address

[§]S.R.-R.: Procter & Gamble, Innovation Center, Strombeek Bever, Belgium.

Notes

The authors declare no competing financial interest.

ACKNOWLEDGMENTS

This work was made possible by the generous financial support of the Ministerio de Economía y Competitividad (MINECO, Project CTQ2011-28124). We also thank the Supercomputing Center of Galicia (CESGA) for computer support.

REFERENCES

(1) *Chiral Analysis*; Busch, K. W., Busch, M. A., Eds.; Elsevier: Amsterdam, 2006.

(2) Bringmann, G.; Bruhn, T.; Maksimenka, K.; Hemberger, Y. *Eur. J. Org. Chem.* **2009**, *2009*, 2717−2727.

(3) Mori, T.; Inoue, Y.; Grimme, S. *J. Org. Chem.* **2006**, *71*, 9797−9806.

(4) Stephens, P. J.; Devlin, F. J.; Cheeseman, J. R. *VCD Spectroscopy For Organic Chemists*; CRC Press: Boca Raton, FL, 2012.

(5) Nicu, V. P.; Baerends, E. J.; Polavarapu, P. L. *J. Phys. Chem. A* **2012**, *116*, 8366−8373.

(6) Devlin, F. J.; Stephens, P. J.; Cheeseman, J. R.; Frisch, M. J. *J. Am. Chem. Soc.* **1996**, *118*, 6327−6328.

(7) Aamouche, A.; Devlin, F. J.; Stephens, P. J. *Chem. Commun.* **1999**, 361−362.

(8) Aamouche, A.; Devlin, F. J.; Stephens, P. J.; Drabowicz, J.; Bujnicki, B.; Mikolajczyk, M. *Chem.—Eur. J.* **2000**, *6*, 4479−4486.

(9) Aamouche, A.; Devlin, F. J.; Stephens, P. J. *J. Am. Chem. Soc.* **2000**, *122*, 7358−7367.

(10) Stephens, P. J.; Davlin, F. J. *Chirality* **2000**, *12*, 172−179.

(11) Stephens, P. J.; Aamouche, A.; Devlin, F. J.; Superchi, S.; Donnoli, M. I.; Rosini, C. *J. Org. Chem.* **2001**, *66*, 3671−3677.
(12) Devlin, F. J.; Stephens, P. J.; Scafato, P.; Superchi, S.; Rosini, C. *Tetrahedron: Asymmetry* **2001**, *12*, 1551−1558.
(13) Devlin, F. J.; Stephens, P. J.; Scafato, P.; Superchi, S.; Rosini, C. *Chirality* **2002**, *14*, 400−406.
(14) Devlin, F. J.; Stephens, P. J.; Osterle, C.; Wiberg, K. B.; Cheeseman, J. R.; Frisch, M. J. *J. Org. Chem.* **2002**, *67*, 8090−8096.
(15) Freedman, T. B.; Cao, X. L.; Dukor, R. K.; Nafie, L. A. *Chirality* **2003**, *15*, 743−758.
(16) Cere, V.; Peri, F.; Pollicino, S.; Ricci, A.; Devlin, F. J.; Stephens, P. J.; Gasparrini, F.; Rompietti, R.; Villani, C. *J. Org. Chem.* **2005**, *70*, 664−669.
(17) Stephens, P. J.; McCann, D. M.; Devlin, F. J.; Flood, T. C.; Butkus, E.; Stoncius, S.; Cheeseman, J. R. *J. Org. Chem.* **2005**, *70*, 3903−3913.
(18) Devlin, F. J.; Stephens, P. J.; Besse, P. *Tetrahedron: Asymmetry* **2005**, *16*, 1557−1566.
(19) Devlin, F. J.; Stephens, P. J.; Bortolini, O. *Tetrahedron: Asymmetry* **2005**, *16*, 2653−2663.
(20) Carosati, E.; Cruciani, G.; Chiarini, A.; Budriesi, R.; Ioan, P.; Spisani, R.; Spinelli, D.; Cosimelli, B.; Fusi, F.; Frosini, M.; Matucci, R.; Gasparrini, F.; Ciogli, A.; Stephens, P. J.; Devlin, F. J. *J. Med. Chem.* **2006**, *49*, 5206−5216.
(21) Stephens, P. J.; McCann, D. M.; Devlin, F. J.; Smith, A. B., III *J. Nat. Prod.* **2006**, *69*, 1055−1064.
(22) Stephens, P. J.; Devlin, F. J.; Gasparrini, F.; Ciogli, A.; Spinelli, D.; Cosimelli, B. *J. Org. Chem.* **2007**, *72*, 4707−4715.
(23) Stephens, P. J.; Pan, J.-J.; Devlin, F. J.; Urbanová, M.; Hájíček, J. *J. Org. Chem.* **2007**, *72*, 2508−2524.
(24) Krohn, K.; Gehle, D.; Dey, S. K.; Nahar, N.; Mosihuzzaman, M.; Sultana, N.; Sohrab, M. H.; Stephens, P. J.; Pan, J.-J.; Sasse, F. *J. Nat. Prod.* **2007**, *70*, 1339−1343.
(25) Stephens, P. J.; Pan, J.-J.; Krohn, K. *J. Org. Chem.* **2007**, *72*, 7641−7649.
(26) Stephens, P. J.; Pan, J. J.; Devlin, F. J.; Krohn, K.; Kurtan, T. *J. Org. Chem.* **2007**, *72*, 3521−3536.
(27) Lattanzi, A.; Scettri, A.; Zanasi, R.; Devlin, F. J.; Stephens, P. J. *J. Org. Chem.* **2010**, *75*, 2179−2188.
(28) Ji, Z.; Santamaria, R. N.; Garzón, I. L. *J. Phys. Chem. A* **2010**, *114*, 3591−3601.
(29) Abbate, S.; Lebon, F.; Lepri, S.; Longhi, G.; Gangemi, R.; Spizzichino, S.; Bellachioma, G.; Ruzziconi, R. *ChemPhysChem* **2011**, *12*, 3519−3523.
(30) Pandith, A. H.; Islam, N.; Syed, Z. F.; Rehman, S.-u.; Bandaru, S.; Anoop, A. *Chem. Phys. Lett.* **2011**, *516*, 199−203.
(31) Sato, H.; Uno, H.; Nakano, H. *Dalton Trans.* **2011**, *40*, 1332−1337.
(32) Moreno, J. R. A.; Ureña, F. P.; González, J. J. L.; Gámez, F.; Martínez-Haya, B. *Tetrahedron: Asymmetry* **2012**, *23*, 294−299.
(33) Wu, T.; Zhang, X.-P.; Li, C.-H.; Bouř, P.; Li, Y.-Z.; You, X.-Z. *Chirality* **2012**, *24*, 451−458.
(34) Zhu, P.; Yang, G.; Poopari, M. R.; Bie, Z.; Xu, Y. *ChemPhysChem* **2012**, *13*, 1272−1281.
(35) Davies, H. M. L.; Beckwith, R. E. J. *Chem. Rev.* **2003**, *103*, 2861−2903.
(36) Doyle, M. P.; Duffy, R.; Ratnikov, M.; Zhou, L. *Chem. Rev.* **2010**, *110*, 704−724.
(37) Davies, H. M. L.; Loe, O. *Synthesis* **2004**, 2595−2608.
(38) Davies, H. M. L.; Nikolai, J. *Org. Biomol. Chem.* **2005**, *3*, 4176−4187.
(39) Fraile, J. M.; Garcia, J. I.; Mayoral, J. A.; Roldan, M. *Org. Lett.* **2007**, *9*, 731−733.
(40) Fraile, J. M.; Mayoral, J. A.; Ravasio, N.; Roldan, M.; Sordelli, L.; Zaccheria, F. *J. Catal.* **2011**, *281*, 273−278.
(41) Fraile, J. M.; Lopez-Ram-de-Viu, P.; Mayoral, J. A.; Roldan, M.; Santafe-Valero, J. *Org. Biomol. Chem.* **2011**, *9*, 6075−6081.
(42) Davies, H. M. L.; Hansen, T.; Churchill, M. R. *J. Am. Chem. Soc.* **2000**, *122*, 3063−3070.
(43) Suematsu, H.; Katsuki, T. *J. Am. Chem. Soc.* **2009**, *131*, 14218−14219.
(44) Davies, H. M. L.; Ren, P. D. *Tetrahedron Lett.* **2001**, *42*, 3149−3151.
(45) Jimenez-Oses, G.; Aydillo, C.; Busto, J. H.; Zurbano, M. M.; Peregrina, J. M.; Avenoza, A. *J. Org. Chem.* **2007**, *72*, 5399−5402.
(46) Aydillo, C.; Jimenez-Oses, G.; Busto, J. H.; Peregrina, J. M.; Zurbano, M. M.; Avenoza, A. *Chem.—Eur. J.* **2007**, *13*, 4840−4848.
(47) Reider, P. J.; Conn, R. S. E.; Davis, P.; Grenda, V. J.; Zambito, A. J.; Grabowski, E. J. J. *J. Org. Chem.* **1987**, *52*, 3326−3334.
(48) Park, H.-g.; Lee, J.; Kang, M. J.; Lee, Y.-J.; Jeong, B.-S.; Lee, J.-H.; Yoo, M.-S.; Kim, M.-J.; Choi, S.-h.; Jew, S.-s. *Tetrahedron* **2004**, *60*, 4243−4249.
(49) Kuppens, T.; Bultinck, P.; Langenaeker, W. *Drug Discovery Today: Technol.* **2004**, *1*, 269−275.
(50) Hansen, J.; Autschbach, J.; Davies, H. M. L. *J. Org. Chem.* **2009**, *74*, 6555−6563.
(51) Garcia, J. I.; Jimenez-Oses, G.; Mayoral, J. A. *Chem.—Eur. J.* **2011**, *17*, 529−539.
(52) Braga, A. A. C.; Maseras, F.; Urbano, J.; Caballero, A.; Díaz-Requejo, M. M.; Pérez, P. J. *Organometallics* **2006**, *25*, 5292−5300.
(53) Bonge, H. T.; Hansen, T. *Eur. J. Org. Chem.* **2010**, *2010*, 4355−4359.
(54) Nakamura, E.; Yoshikai, N.; Yamanaka, M. *J. Am. Chem. Soc.* **2002**, *124*, 7181−7192.
(55) Wang, J.; Chen, B.; Bao, J. *J. Org. Chem.* **1998**, *63*, 1853−1862.
(56) Davies, H. M. L.; Jin, Q. H.; Ren, P. D.; Kovalevsky, A. Y. *J. Org. Chem.* **2002**, *67*, 4165−4169.
(57) Mbuvi, H. M.; Woo, L. K. *Organometallics* **2008**, *27*, 637−645.
(58) Fraile, J. M.; Garcia, J. I.; Martinez-Merino, V.; Mayoral, J. A.; Salvatella, L. *J. Am. Chem. Soc.* **2001**, *123*, 7616−7625.
(59) Fraile, J. M.; Garcia, J. I.; Gil, M. J.; Martinez-Merino, V.; Mayoral, J. A.; Salvatella, L. *Chem.—Eur. J.* **2004**, *10*, 758−765.
(60) Grimme, S.; Antony, J.; Ehrlich, S.; Krieg, H. *J. Chem. Phys.* **2010**, *132*, 154104.
(61) Cornejo, A.; Fraile, J. M.; Garcia, J. I.; Gil, M. J.; Martinez-Merino, V.; Mayoral, J. A.; Pires, E.; Villalba, I. *Synlett* **2005**, 2321−2324.
(62) Fraile, J. M.; Garcia, J. I.; Herrerias, C. I.; Mayoral, J. A.; Reiser, O.; Socuellamos, A.; Werner, H. *Chem.—Eur. J.* **2004**, *10*, 2997−3005.
(63) Glos, M.; Reiser, O. *Org. Lett.* **2000**, *2*, 2045−2048.
(64) Werner, H.; Vicha, R.; Gissibl, A.; Reiser, O. *J. Org. Chem.* **2003**, *68*, 10166−10168.
(65) Lee, C.; Yang, W.; Parr, R. G. *Phys. Rev. B* **1988**, *37*, 785−789.
(66) Becke, A. D. *J. Chem. Phys.* **1993**, *98*, 5648−5652.
(67) Harihara, Pc.; Pople, J. A. *Theor. Chim. Acta* **1973**, *28*, 213−222.
(68) Marenich, A. V.; Cramer, C. J.; Truhlar, D. G. *J. Phys. Chem. B* **2009**, *113*, 6378−6396.
(69) Frisch, M. J.; et al. *Gaussian 09*; Gaussian, Inc.: Wallingford, CT, 2009.